

Isotropic Wavelets: a Powerful Tool to Extract Point Sources from CMB Maps

L. Cayón¹, J.L. Sanz^{1,2}, R.B. Barreiro^{1,3,4}, E. Martínez-González¹, P. Vielva^{1,3},

L. Toffolatti⁵, J. Silk⁶, J.M. Diego^{1,3} & F. Argüeso⁷

1. *Instituto de Física de Cantabria, Fac. Ciencias, Av. los Castros s/n, 39005 Santander, Spain*

2. *On sabbatical leave at Center for Particle Astrophysics and Astronomy Department, University of California, Berkeley, USA*

3. *Departamento de Física Moderna, Universidad de Cantabria, 39005 Santander, Spain.*

4. *Astrophysics Group, Cavendish Laboratory, Madingley Road, Cambridge CB3 0HE, UK*

5. *Dpto. de Física, Universidad de Oviedo, c/ Calvo Sotelo s/n, 33007 Oviedo, Spain*

6. *Astronomy Department, University of Oxford, UK*

7. *Dpto. de Matemáticas, Universidad de Oviedo, c/ Calvo Sotelo s/n, 33007 Oviedo, Spain*

1 May 2018

ABSTRACT

It is the aim of this paper to introduce the use of isotropic wavelets to detect and determine the flux of point sources appearing in CMB maps. The most suited wavelet to detect point sources filtered with a Gaussian beam is the Mexican Hat. An analytical expression of the wavelet coefficient obtained in the presence of a point source is provided and used in the detection and flux estimation methods presented. For illustration the method is applied to two simulations (assuming Planck Mission characteristics) dominated by CMB (100 GHz) and dust (857 GHz) as these will be the two signals dominating at low and high frequency respectively in the Planck channels. We are able to detect bright sources above 1.58 Jy at 857 GHz (82% of all sources) and above 0.36 Jy at 100 GHz (100% of all) with errors in the flux estimation below 25%. The main advantage of this method is that nothing has to be assumed about the underlying field, i.e. about the nature and properties of the signal plus noise present in the maps. This is not the case in the detection method presented by Tegmark and Oliveira-Costa 1998. Both methods are compared producing similar results.

Key words: cosmology: CMB – data analysis

1 INTRODUCTION

One of the major challenges in the study of the Cosmic Microwave Background (CMB) at present, is to overcome the problem of separating the cosmological signal from the Galactic foreground emissions, the noise and the extragalactic point sources, in the future high resolution CMB maps. Such missions as MAP (Bennett et al. 1996) and Planck (Mandolesi et al. 1998; Puget et al. 1998) will produce CMB maps that will be seriously affected by this problem.

Several methods have already been tested to perform the separation of the different emissions in CMB observations, as the ones based on the Wiener filter (Tegmark and Efstathiou 1996, Bouchet and Gispert 1999) and on Maximum Entropy Methods (Hobson et al. 1998, 1999). Recently, wavelet techniques have been introduced in the analysis of CMB data. Denoising of CMB maps has been performed on patches of the sky of $12^\circ.8 \times 12^\circ.8$ using multiresolution

techniques (Sanz et al. 1999a) and 2D wavelets (Sanz et al. 1999b), as well as on the whole celestial sphere (Tenorio et al. 1999).

Extragalactic point sources should be removed from the maps before any analysis is performed. There are still many uncertainties regarding the composition of this population, the characteristics of the sources, and their time variability as well as the abundance and emission at different frequencies. Simulations of the emission of extragalactic sources at the observing frequencies of the Planck mission have been worked out by Toffolatti et al. 1998 and Guiderdoni 1999. In general there is agreement between these extrapolations. In this paper we use simulations based on the predictions of Toffolatti et al. 1998. The number counts of bright objects at frequencies above 300 GHz are dominated by far-IR selected sources. Lower frequencies will get most of the emission from radio selected sources.

Removal of point sources in the observed maps is usu-

ally done by removing all pixels above a threshold of 5σ . The error in rejecting pixels not corresponding to point sources is very small. However, large number of point sources will still remain undetected. Tegmark and Oliveira-Costa 1998 (TOC98 hereinafter) presented a method to locate and detect point sources based on the minimization of the variance of the map. The application of this technique assumes that the CMB, noise and Galactic foregrounds behave as Gaussian fields and it requires knowledge of the power spectrum of these components. As a product of the MEM used to separate all the foreground components from the CMB, Hobson et al. 1999 are able to recover the point sources present in the simulated maps included as part of the noise in the method. However they are not able to remove the brightest sources that can still be observed in the residuals. As will be shown these will be the point sources that the method presented here is able to extract. Tenorio et al. 1999 applied Daubechies wavelets to detect and remove point sources from CMB plus noise flat maps. However Daubechies wavelets are not the optimal ones to detect point sources as explained below. As part of the effort to explore the possibilities of using wavelets to extract the information contained in CMB observations, we are studying in this paper isotropic wavelets in the context of this data. In particular, taking advantage of the spherical symmetry, these wavelets are very appropriate for locating and detecting point sources. The method does not assume any behaviour for the rest of the signals and noise present in the maps. The basic point source characteristics are its Gaussian shape and scale, defined by the beam used in the observations. Convolution of the CMB map with a wavelet of the same scale and similar shape of the point source will produce wavelet coefficients with maxima (amplification) at the position of point sources (location). The most appropriate wavelet to detect Gaussian shaped sources is the so called Mexican Hat. This wavelet has been used to detect sources in the presence of noise in X-ray images by Damiani et al. 1997.

The paper is organized as follows. An analytical approach to the use of isotropic wavelets to analyse CMB maps is presented in section 2. Section 3 is dedicated to the application of isotropic wavelets to CMB maps in order to detect point sources. A comparison with the TOC98 method is also included in this section. We present the flux estimation of the detected point sources in section 4. Wherever flux magnitudes are given they refer to the total integrated flux under the beam. Conclusions are included in section 5.

2 ANALYTICAL APPROACH

The continuous isotropic wavelet transform of a 2D signal $f(\vec{x})$ is defined as

$$wv(R, \vec{b}) = \int d\vec{x} f(\vec{x}) \Psi(R, \vec{b}; \vec{x}),$$

$$\Psi(R, \vec{b}; \vec{x}) = \frac{1}{R} \psi\left(\frac{|\vec{x} - \vec{b}|}{R}\right), \quad (1)$$

where $wv(R, \vec{b})$ is the wavelet coefficient associated with the scale R at the point with coordinates \vec{b} . $\psi(|\vec{x}|)$ is the ‘‘mother’’ wavelet that is assumed to be isotropic and satisfies the constraint $\int d\vec{x} \psi = 0$, $\int d\vec{x} \psi^2 = 1$ and the admis-

sibility condition: $C_\psi = (2\pi)^2 \int_0^\infty dk k^{-1} \psi^2(k) < \infty$, where $\psi(k)$ is the Fourier transform of $\psi(x)$. This is a necessary and sufficient condition in order to synthesise the function with the wavelet coefficients

$$f(\vec{x}) = \frac{1}{C_\psi} \int dR d\vec{b} \frac{1}{R^4} wv(R, \vec{b}) \psi\left(\frac{|\vec{x} - \vec{b}|}{R}\right). \quad (2)$$

Our aim is to locate point sources in microwave maps. The wavelet coefficients given by equation (1), provide information about the contribution of different scales (R) to the value of the analyzed function (f) at a certain location (\vec{b}). Moreover, they will increase as the shape of the wavelet (Ψ) gets closer to the shape of the analyzed function. We want to maximize the wavelet coefficients at the location of point sources. As observations are performed through antennas, the observed point sources will be the result of a convolution with a certain antenna response function. The response is most frequently modeled as a Gaussian. The most appropriate isotropic wavelet to use in this case is the so called Mexican Hat wavelet given by:

$$\psi(x) = (2\pi)^{-1/2} (2 - x^2) e^{-x^2/2}. \quad (3)$$

The convolution of the Mexican Hat wavelet with an image consistent of point sources filtered with a Gaussian beam, is a functional proportional to the second derivative of the analyzed function and therefore related to the maxima and minima in the analyzed image. Moreover the wavelet coefficients corresponding to a constant background will be identically zero. We would also like to point out the resemblance between the Mexican Hat wavelet and the filter used in TOC98 who obtained the optimal filter to detect point sources.

Observations of the CMB contain not only the cosmological CMB signal but also Galactic emission (synchrotron, free-free and dust), noise and extragalactic emission (Sunyaev-Zeldovich effect and point sources). We are interested in removing point sources (some of the Sunyaev-Zeldovich sources will be extended and we will deal with the removal of these in a future paper) from the underlying signal (CMB or Galactic emissions) plus noise image. If one assumes that the sources that will appear in real maps at different frequencies correspond to the convolution of a point source with a Gaussian of dispersion σ_a (antenna beamwidth), then any source (we are only concerned with the detection of point sources in this paper and will therefore use the word source to refer to the filtered point sources unless otherwise indicated) can be represented by a function: $f(\vec{x}) = (B/A) e^{-(\vec{x} - \vec{x}_o)^2 / 2\sigma_a^2}$, B being the flux of the point source and A the area under the beam. At the position of the peak of the source one has the following wavelet coefficient at scale R :

$$\frac{wv(R, \vec{x}_o)}{R} = 2(2\pi)^{1/2} (B/A) x(1+x)^{-2}, \quad x \equiv \left(\frac{R}{\sigma_a}\right)^2, \quad (4)$$

whereas the wavelet variance of the signal plus noise at scale R is given by the expression

$$\frac{\sigma_{wv}^2(R)}{R^2} = 4\pi\sigma_s^2 \left[\frac{(\sigma_p/R)^2}{SNR^2} + \frac{\Gamma(\frac{n+7}{2})}{2\Gamma(\frac{n+3}{2})} \frac{x^2}{(1+x)^{\frac{n+7}{2}}} \right], \quad (5)$$

where σ_s, σ_p are respectively the signal dispersion in real space and the pixel scale $\sigma_p = l_p/2\pi$ (l_p being the pixel size),

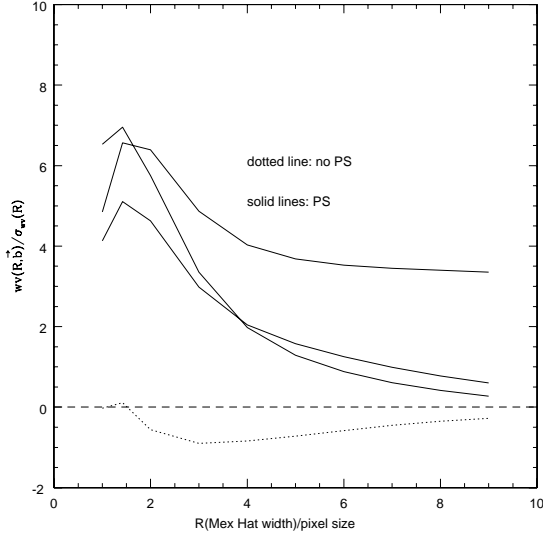


Figure 1. Wavelet coefficients normalized to the dispersion of the wavelet coefficient map as a function of the Mexican Hat width R in units of number of pixels. Each of the curves corresponds to different locations in the analyzed map (different pixels in the original map that includes signal (dust), noise and point sources). Pixels occupied by a point source are represented by solid lines. The dotted line corresponds to a pixel where there is no point source.

and it is assumed that $R \gg \sigma_p$. SNR is the signal to noise ratio of the signal plus noise map. The signal has been represented by a power spectrum with effective index n . Consider the amplification suffered by the flux of a source as the ratio of the detection level in wavelet space ($wv(R, \vec{x}_o)/\sigma_{wv}(R)$) to the detection level in real space ($(B/A)/\sigma_{s+n}$). This quantity will be maximum at $R \simeq \sigma_a$ as the wavelet at that scale selects the contribution of scales around the size of the source whereas the signal and noise appear at a higher or lower scale, respectively. In theory, one can calculate the amplification taking into account equations (4) and (5). The amplification factor is obtained to be greater than 2.3 for CMB dominated maps and larger in the case of dust dominated maps. This result is also obtained numerically as will be shown in the next section.

3 POINT SOURCE DETECTION

Isotropic wavelets are defined as a function of position \vec{b} and scale R . As pointed out in the previous section, the optimal wavelet scale in order to detect point sources in CMB maps is approximately the dispersion of the antenna $\simeq \sigma_a$. Convolution with a Mexican Hat of that scale will produce peaks at the positions of point sources and will allow for point source detection.

Our aim is to illustrate the performance of the detection technique considering representative maps of high sensitivity experiments. We have chosen to simulate maps following the Planck Mission characteristics. The detection method is applied to simulations of flat patches of the sky of $12^\circ.8 \times 12^\circ.8$ at two different frequencies, 100 and 857 GHz, with angular resolution (arcmin)=10 (100 GHz), 5 (857 GHz) and pixel

size (arcmin)=3 (100 GHz), 1.5 (857 GHz). As previously pointed out, CMB observations will contain the cosmological signal, Galactic foregrounds emissions, extragalactic emissions and instrumental noise. In the frequency range that the Planck Mission will sample, the observed maps will be dominated either by the cosmological CMB signal at low frequencies (below ~ 200 GHz) or by dust at high frequencies. As two representative extreme cases we have chosen 100 and 857 GHz to present the detection method based on isotropic wavelets. Therefore simulations at 100 GHz include cosmological signal, point sources and instrumental noise and simulations at 857 GHz consist of dust emission, point sources and instrumental noise. Cosmological signal simulations are performed of Cold Dark Matter (CDM) model with $\Omega = 1$. Dust simulations are made using the predicted full-sky maps of Finkbeiner et. al. 1999. These predictions assume that dust emission corresponds to two grey bodies, with an emissivity of 1.67 for the cold one and 2.70 for the hot one (this has been checked in the frequency range of FIRAS). Point source simulations at the two frequencies considered are based on the code developed by Toffolatti et al. 1998. Non correlated Gaussian noise is added to the signal with a $\Delta T/T$ per resolution element of 4.3×10^{-6} at 100 GHz and 6670×10^{-6} at 857 GHz as in the corresponding two channels of the Planck mission.

To show how different Mexican Hat widths affect the value of the wavelet coefficients at positions in the simulated map with or without a point source, we have plotted in Figure 1 the value of the wavelet coefficient normalized to the dispersion of the wavelet coefficient map as a function of the Mexican Hat width R . It is clear that pixels with a point source have a characteristic curve with a maximum at $R \simeq \sigma_a$. Taking this behaviour into account, the detection method proceeds in three steps. First the simulated map is convolved with Mexican Hat wavelets of several widths (R) obtaining maps of wavelet coefficients at each R . In the second step we look at the map of wavelet coefficients obtained for $R = \sigma_a$ (scale at which the amplification is maximum) and find the spots (connected pixels) appearing above $5\sigma_{wv}(R = \sigma_a)$. The location of the maxima of these spots will correspond to the location of point sources as previously discussed. In order to make sure that all detections correspond to real point sources we determine, in the third step, the numerical curve of $wv(R, \vec{x}_o)/\sigma_{wv}(R)$ as a function of R (being \vec{x}_o the position of a maximum identified in the second step) and compare it with the theoretical one given by equations (4) and (5). A reduced χ^2 is calculated and only maxima positions with values of $\chi^2 \approx 1$ are accepted as point source detections.

We have plotted in Figure 2 the number of point sources detected above a certain flux together with the number of point sources that exist in the simulation after filtering (notice that the number of point sources above a certain flux can change when a Gaussian filter is applied to the simulated map, in particular at high frequencies and low fluxes). As one can see the detected point sources are the ones with the highest fluxes. The method is best suited to detect the bright sources leaving the majority of the faint ones undetected. At 857 GHz the number of point sources detected using the wavelet method is 82% of the ones that exist in the simulation with fluxes above 1.58 Jy. At 100 GHz we are able to detect 100% of all the point sources existing above

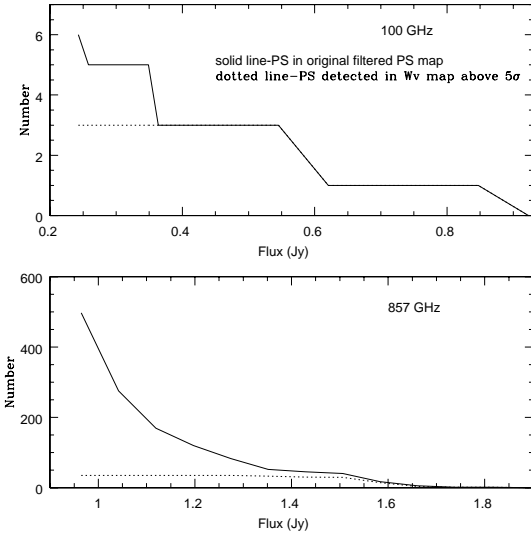


Figure 2. In each of the two panels the dotted line shows the number of point sources detected by the Wavelet method above a given threshold. The number of simulated sources after filtering with a Gaussian beam of $FWHM = 10', 5'$ at 100 and 857 GHz respectively, is indicated by a solid line. Top and bottom figures correspond to the simulations at 100 and 857 GHz respectively.

0.36 Jy. We have also looked at the amplification suffered by the detected point sources (once the point source is located we compare the amplitude of that pixel in the wavelet coefficients map relative to the dispersion of that map with the amplitude of that pixel in the original (signal plus noise plus point sources) map relative to the dispersion of that map) obtaining average values of 11 and 4 at 857 GHz and 100 GHz respectively.

We have compared our results with the method used in TOC98. To illustrate how both methods perform on the same data we have considered the same simulations at 100 GHz and 857 GHz. The number of point sources detected by the two methods are given in Table 1 (also included in the second column is the number of point sources directly found above 5σ in the signal plus noise plus point sources map). As one can see, the performance of both methods is comparable. Moreover the average amplification suffered by the detected point sources is also comparable. The detection is clearly improved in relation to considering only peaks above 5σ . This improvement is a consequence of the amplification suffered by the amplitude of the point sources after applying the Mexican Hat wavelet (with the appropriate scale). It is important to note that no assumptions about the nature of the underlying signal plus noise field are made in the wavelet method presented in this paper. However, the detection method of TOC98 is based on modeling the signal plus noise present in the analyzed maps as Gaussian random fields and requires a knowledge of the power spectrum of all of the signal plus the noise components.

Table 1. Number of point sources detected above 5σ and using the wavelet and the TOC98 methods

Frequency (GHz)	Above 5σ	Wavelet	TOC98
857	8	35	32
100	0	3	3

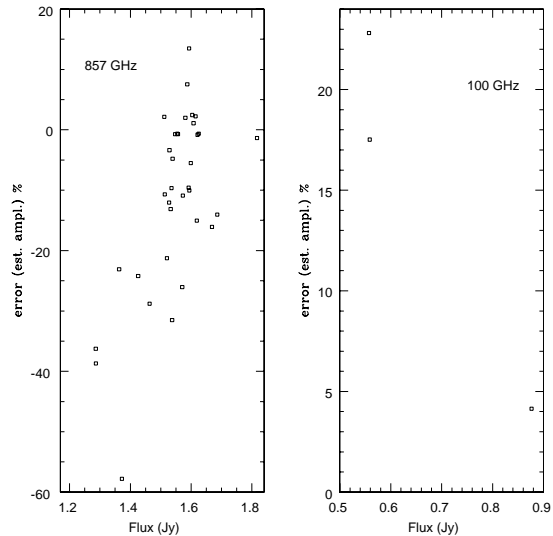


Figure 3. Error in the estimated flux of the point sources detected at 857 and 100 GHz (left and right panels respectively) as a function of the input flux.

4 FLUX ESTIMATION OF THE DETECTED POINT SOURCES

In this section we want to show how the flux of the detected point sources can be recovered using wavelet coefficients. From equation (4) we know the analytical expression of the wavelet coefficient at the position of the detected point source, being proportional to the filtered flux of the point source B . Moreover, to take into account the information at different scales we obtain the final amplitude value from the χ^2 fit presented in section 3. Defining the error in the flux estimation as the ratio of the difference between the real and the recovered value divided by the real value, we have plotted in Figure 3 these errors for the point sources detected in the two simulated maps. At 857 GHz point sources with fluxes above 1.58 Jy have errors with absolute values below 20%, and 46% of all detections have errors with absolute values below 10%. The three point sources detected at 100 GHz have errors with absolute values below 25%. As one can see from the figure the overestimated amplitudes have larger errors than the underestimated ones (this can only be seen in the 857 GHz results as the statistics of detected point sources is very poor at 100 GHz). There is also a slight bias towards negative error values. The χ^2 fit used to recover the amplitude does not take into account possible correlations between the different scales. Including these correlations improves the amplitude determination method so that no bias appears. This will be presented in a future paper.

Once the position and the flux of the detected point sources is known, one can simulate a map with only point sources filtered with the corresponding Gaussian beam (depending on the frequency) and subtract it from the original map. A map with point sources removed will be obtained. This will be an improvement on the map obtained by setting to 0 the value of the pixels affected by the detected point sources as is usually done.

5 CONCLUSIONS

Wavelet coefficients provide information at each location of an analyzed image of the contributions from the different scales. Moreover, as they are obtained from the convolution of the image with the wavelet, in the case that the shape of the wavelet coincides with the shape of the field at a fixed position, the wavelet coefficient will be maximum. Since we are interested in extracting point sources from CMB maps, isotropic wavelets have the appropriate shape. CMB observations are performed using antennas with a characteristic response. Modeling the antenna as a Gaussian beam the observed point sources will be the result of convolving with such a beam. In this case, the best suited isotropic wavelet to detect point sources is the Mexican Hat. This wavelet has a very similar shape to the optimal filter used by TOC98.

As a demonstration of the method, the study is performed on simulations at 100 GHz and 857 GHz dominated by CMB and dust respectively and with the characteristics of the future Planck Mission. We have used the Mexican Hat wavelet to detect and determine the flux of point sources in 12.8×12.8 square degree simulations. The detection method is based on the maxima reached by the wavelet coefficients at $R \simeq \sigma_a$ at point source positions. The reason for this is that the signal and the noise have characteristic scales larger and smaller than σ_a respectively and the wavelet used has the appropriate shape to resemble that of a point source filtered with a Gaussian. We consider detections above $5 \sigma_{wv}(R = \sigma_a)$. Making use of the information provided by the wavelet coefficients obtained convolving with Mexican Hat wavelets of different widths (R) as well as of the analytical expression we make sure that all detections correspond to real point sources by a reduced χ^2 fit. This method detects point sources in the simulated maps above ≈ 1.2 Jy at 857 GHz and above ≈ 0.5 Jy at 100 GHz. 82% of the existing point sources above 1.58 Jy are detected in the simulation at 857 GHz whereas all the existing point sources above 0.36 Jy are detected at 100 GHz. The detections are achieved due to the amplification suffered by the ratio of the flux of the point source in the wavelet coefficient map (at $R = \sigma_a$) relative to the dispersion of that map in comparison with the flux in the original simulated map relative to its dispersion. Average amplification values of 11 and 4 are found at 857 GHz and 100 GHz. It is very important to note that the detection method is not based on any assumption about the nature of the signal plus noise. The method presented in TOC98 provides comparable results as presented in section 3. TOC98 method uses the optimal filter to locate point sources in CMB maps however a price has to be paid: the signal and noise are assumed to be Gaussian random fields and a knowledge of the power spectrum is required. We would also like to point out the possibility of using this method

as complementary to the MEM presented in Hobson et al. 1999. The bright point sources could be removed from the maps before MEM is applied. The rest of the point sources still in the analyzed maps will be recovered as a product of the separation method as explained in their paper.

Finally, based on the analytical knowledge of the wavelet coefficients at positions dominated by point sources we recover the flux of the detected point sources. For the extracted point sources with fluxes above 1.58 Jy at 857 GHz the errors (absolute value) are below 20%. The flux of the point sources detected in the simulation at 100 GHz have errors (absolute value) below 25%. Removal of these point sources from the original map can therefore be done by simulating maps of only point sources at the locations found in the detection procedure and subtracting them from the initial ones. We would also like to point out that an analysis of the whole sphere could also be performed by just dividing the sphere in small flat patches.

This paper is aimed to serve as a presentation of the power of isotropic wavelets to detect sources in CMB maps. No information on different frequencies has been used in this work. In a future paper we will add this information and will study the separation of Sunyaev-Zeldovich sources from point sources in Planck simulated maps.

ACKNOWLEDGMENTS

This work has been supported by the Comisión Conjunta Hispano-Norteamericana de Cooperación Científica y Tecnológica ref. 98138, Spanish DGES Project no. PB95-1132-C02-02, Spanish CICYT Acción Especial no. ESP98-1545-E and the EEC project INTAS-OPEN-97-1992. L.C. thanks the CfPA hospitality during May 1999. J.L.S. acknowledges partial financial support from a Spanish MEC fellowship and CfPA and thanks Berkeley Astronomy Dept. hospitality during year 1999. R.B.B. thanks financial support from Spanish MEC in the form of a predoctoral fellowship and from the PPARC in the form of a research grant. PV acknowledges support from an Universidad de Cantabria fellowship. LT acknowledges partial financial support from the Italian ASI and CNR. JMD acknowledges support from a Spanish MEC fellowship FP96 20194004.

REFERENCES

- Bennett, C. et al. 1996; MAP homepage <http://map.gsfc.nasa.gov>
- Bouchet, F.R. & Gispert, R. 1999, astro-ph/9903176
- Damiani, F., Maggio, A., Micela, G. & Sciortino, S. 1997, ApJ, 483, 350
- Finkbeiner, D.P., Davis, M. & Schlegel, D.J. 1999, astro-ph/9905128
- Guiderdoni, B. 1999, astro-ph/9903112
- Hobson, M.P., Jones, A.W., Lasenby, A.N. & Bouchet, F.R. 1998, MNRAS, 300, 1.
- Hobson, M.P., Barreiro, R.B., Toffolatti, L., Lasenby, A.N., Sanz, J.L., Jones, A.W. & Bouchet, F.R. 1999, MNRAS, 306, 232.
- Mandolesi, N. et al. 1998; Proposal submitted to ESA for the Planck Low Frequency Instrument
- Puget, J.L. et al. 1998; Proposal submitted to ESA for the Planck High Frequency Instrument
- Sanz, J.L., Argüeso, F., Cayón, L., Martínez-González, E., Barreiro, R.B. & Toffolatti, L. 1999a, MNRAS, 309, 672.

- Sanz, J.L., Barreiro, R.B., Cayón, L., Martínez-González, E., Ruiz, G.A., Díaz, F.J., Argüeso, F., Silk, J. & Toffolatti, L. 1999b, *A&AS*, 140, 99.
- Tegmark, M. & Efstathiou, G. 1996, *MNRAS*, 281, 1297
- Tegmark, M. & Oliveira-Costa, A. 1998, *ApJ*, 500, 83
- Tenorio, L., Jaffe, A.H., Hanany, S. & Lineweaver, C.H. 1999, astro-ph/9903206.
- Toffolatti, L. et al. 1998, *MNRAS*, 297, 117